

Single Injection Earth Return Trajectory Options for Small Spacecraft Missions to the Moon

Cesar Ocampo, Assistant Professor
Department of Aerospace Engineering & Engineering Sciences
The University of Texas at Austin
(512) 471-5696
cesar.ocampo@mail.utexas.edu

Shawn Hayes, Graduate Student
Department of Aerospace Engineering & Engineering Sciences
The University of Texas at Austin
(512) 471-4332
shawn.hayes@mail.utexas.edu

Robert Twiggs, Professor
Department of Aeronautics and Astronautics
Stanford University
(650) 723-8651
btwiggs@leland.stanford.edu

Abstract. There exist several classes of high energy trajectories that are injected from Earth centered orbits to deep space destinations and return to the vicinity of the Earth sometime later due to the direct influence of a third body perturbation. These trajectories can be designed to flyby the moon or near Earth asteroids and comets. The appealing characteristic of these trajectories is that they require a single injection maneuver at the Earth and no further translational control thereafter. A spacecraft on such a trajectory can take observations and measurements of the flyby body and download the data once it returns to the vicinity of the Earth. The return trajectory could place the spacecraft into a direct reentry path through the Earth's atmosphere or an elliptical or hyperbolic Earth flyby that will be completely passive since no maneuvers are made. This type of trajectory is applicable to passive spacecraft missions such as student built micro satellites that have no on board propulsion for attitude or translational control. Issues addressed are the dispersions in the return trajectory due to errors in the injection maneuver and other orbit parameters. The characteristics of an Earth return lunar flyby mission for small satellites are discussed.

Introduction

Several universities have proposed small satellite projects that will send small spacecraft on the order of 100kg to various locations in cislunar space. Their efforts have been hampered by difficulties securing launch dates and raising the necessary financial resources to support the missions. As a result, progress on some of the missions has been sluggish, not allowing students the opportunity to see the project through from its concept to completion. This in effect, has diminished the hands on experience that these programs were originally designed to give.

Stanford University's Space Systems Development Laboratory (SSDL) identified these issues in its own micro-satellite program and as a result, the CubeSat Project was initiated. This project is unique because it allows students to participate in the mission from concept to completion. The program accomplishes this task by scaling down the satellites. That is, the CubeSats are picosatellites that must be ten centimeter cubes and have a mass less than or equal to one kilogram.

The University of Texas at Austin in partnership with Stanford University intends to take the CubeSat initiative to a higher level by examining the possibility of sending CubeSats to the Moon, near Earth asteroids and comets. This paper is meant as both a catalyst and as a starting point to get other academic institutions excited about the possibilities of such a mission.

This paper focuses on the free return trajectories necessary to successfully complete a lunar CubeSat mission. It also examines the sensitivity of the final Earth return conditions to the injection burn parameters. A discussion

of the extension of the mission design aspects to comet and asteroid flybys is also included.

Earth Return Lunar Flyby

Free Earth return trajectories around the Moon have been studied and used since the Apollo era. The Apollo lunar landing missions used these trajectories to provide a free return and abort option for the human crew. Lunar free return trajectories have also been used to place geostationary bound spacecraft in their proper orbits^{1,2}. This section describes the dynamics and techniques used to compute these trajectories and a method of examining the sensitivity of the solution with respect to perturbations in the injection sequence.

The Force Model

Generally, the fundamental dynamics associated with a spacecraft operating in the Earth-Moon system are studied in a force model that includes; the gravitational attraction from both bodies, additional accelerations due to other third body gravitational attraction, non-spherical gravitational perturbations, atmospheric drag, and solar radiation pressure. Since the small perturbations do not significantly influence the solutions examined here, they can be ignored.

The state vector of the spacecraft relative to an Earth centered equatorial frame is defined as

$$\mathcal{X} = (\mathcal{P}^T \parallel \mathcal{V}^T)^T \quad (1)$$

Where \mathcal{P} is the position vector of the spacecraft with respect to an Earth centered frame and \mathcal{V} is the velocity vector.

The fundamental plane is the equatorial plane of the Earth, and the z-axis points north. The second order vector equation of motion is

$$\mathbf{f} = -\frac{GM_{Earth}}{r^3} \mathbf{r} - \frac{GM_{Moon}}{(\mathbf{r} - \mathbf{r}_{12})^3} (\mathbf{r} - \mathbf{r}_{12}) - \frac{GM_{Moon}}{(r_{12})^3} \mathbf{r}_{12} \quad (2)$$

Where GM_{Earth} is the gravitational parameter of the Earth, GM_{Moon} is the gravitational parameter of the Moon and \mathbf{r}_{12} is the position vector of the Moon relative to the Earth centered equatorial frame.

Note that the last term in Eqn. 2 accounts for the fact that the equations of motion are referenced to the center of the Earth, and not an inertial frame. This is an explicit function of time and is given by a standard lunar ephemeris.

To study the sensitivity of the solutions to perturbations in the state at discrete times it is necessary to linearize perturbations along a nominal solution. The process is as follows. The first order form of the equations of motion are given by

$$\dot{\mathbf{r}} = \mathbf{f} = \begin{pmatrix} \mathbf{f} \\ \mathbf{v} \end{pmatrix} = \begin{pmatrix} \mathbf{r} \\ \mathbf{v} \end{pmatrix} \quad (3)$$

Linearization of perturbations along a solution are given to first order by

$$\delta \mathbf{x}(t) \cong \mathbf{\Phi}(t, t_o) \delta \mathbf{x}(t_o) + \mathbf{X}(t) \delta t \quad (4)$$

where

$$\mathbf{\Phi}(t, t_o) = \frac{\partial \mathbf{f}}{\partial \mathbf{x}} \mathbf{\Phi}(t_o, t_o) = \begin{pmatrix} \mathbf{O}_{3 \times 3} & \mathbf{I}_{3 \times 3} \\ \mathbf{G}_{3 \times 3} & \mathbf{O}_{3 \times 3} \end{pmatrix}_{6 \times 6} \mathbf{\Phi}(t_o, t_o)$$

which is subjected to the initial condition

$$\mathbf{\Phi}(t_o, t_o) = \mathbf{I}_{6 \times 6}$$

Here $\mathbf{\Phi}(t, t_o)$ is the state transition matrix, $\delta \mathbf{x}(t)$ is the contemporaneous state perturbation, $\delta \mathbf{x}(t)$ is the total state differential and $\mathbf{I}_{6 \times 6}$ is a 6 x 6 identity matrix. The state transition matrix is used to map perturbations in position and velocity between discrete times. Along with the first order equation of motion, it forms the set of the variational equations of the system. The \mathbf{G} sub-matrix is a gravity gradient matrix that takes the form

$$\mathbf{G} = -GM_{Earth} \left(-\frac{3}{r^5} \mathbf{r} \mathbf{r}^T + \frac{1}{r^3} \mathbf{I}_{3 \times 3} \right) - GM_{Moon} \left(-\frac{3}{\tilde{r}^5} \tilde{\mathbf{r}} \tilde{\mathbf{r}}^T + \frac{1}{\tilde{r}^3} \mathbf{I}_{3 \times 3} \right) \quad (5)$$

where

$$\tilde{\mathbf{r}} = \mathbf{r} - \mathbf{r}_{12}$$

Finite Burn Model

Spacecraft maneuvers that change the trajectory can be considered impulsive if the duration of an engine burn is short compared to the total mission time. Impulsive maneuvers are then treated as discrete points on the trajectory where the velocity vector and the mass of the spacecraft are changed instantaneously. If the maneuver is not treated impulsively, but rather as a finite burn of a certain duration, then the mass of the vehicle is an additional state variable that is included in the equations of motion. The resulting equations of motion are

$$\mathbf{f} = \begin{pmatrix} \mathbf{r} \\ \mathbf{v} \\ \mathbf{f}(\mathbf{r}) + \frac{T}{m} \mathbf{u} \\ -\frac{T}{c} \end{pmatrix} \quad (7)$$

Where T is the thrust of the engine, \hat{u} is the thrust pointing unit vector and c is the engine's exhaust velocity. The analysis presented here includes results for both the impulsive and finite burn engine models.

Trajectory Identification

To construct a solution that begins at the Earth, flies around the moon, and returns to the Earth, assume the spacecraft is in a parking orbit about the Earth defined by the classical elements ($a, e, i, \Omega, \omega, v$) at an epoch t_o . Assume further that Ω can be adjusted, but the remaining elements are fixed; the fixed elements depend on the launch system that places the spacecraft in Earth orbit. Opting to parameterize position in orbit via a coast time from t_o , instead of using the true anomaly, v , let t_i represent the time the injection maneuver for the translunar injection burn is made. The maneuver is constrained to point along the velocity direction at the point the maneuver is made. With these conditions, a lunar flyby trajectory that returns to the Earth can be produced by choosing as independent variables the vector \hat{a} which is as

$$\hat{a} = (t_o \quad \Omega_o \quad t_i \quad \Delta v \quad t_f)_{1 \times 5}^T \quad (8)$$

The epoch, t_o , is a necessary free parameter that controls' the location of the Moon. Ω_o is necessary because it defines the location of the projection of the line of apsides on the equatorial plane thus allowing the translunar trajectory to point in the correct direction for an encounter with the Moon. Δv is the magnitude of the injection maneuver and t_f is the final time. For the finite engine burn model, the maneuver begins at t_i and the burn duration, Δt_b , is used to control the magnitude of the maneuver. The thrust direction can be chosen to point along the instantaneous velocity vector or held inertially fixed during the maneuver.

Let a subset of the fixed parameters form a constant vector \hat{b} , which is defined by

$$\hat{b} = (a_o \quad e_o \quad i_i \quad \omega_o \quad v_o)_{1 \times 5}^T \quad (9)$$

Where a_o is the semi major axis, e_o is the eccentricity, i_i is inclination, ω_o is the argument of perigee and v_o is the true anomaly.

Finally, let the final constraint vector (the target vector) be the vector \hat{c} , which is defined by

$$\hat{c} = \begin{pmatrix} r_f^* - r_f \\ \dot{r}_f^* - \dot{r}_f \\ h_{xf}^* - h_{xf}^* \\ h_{yf}^* - h_{yf}^* \\ h_{zf}^* - h_{zf}^* \end{pmatrix}_{5 \times 1} \quad (10)$$

Where r_f^* is the desired final radius distance at t_f , \dot{r}_f^* is the desired radial velocity, and h_{xf}^* , h_{yf}^* , h_{zf}^* are the x, y, z components of the angular momentum unit vector. Note that all of these parameters are referenced to the Earth centered equatorial frame.

This constraint vector must be targeted to be zero to obtain a converged solution. The parameters of Eqn. 10 control the final inclination and ascending node. As an example, if it is desired to generate a post lunar flyby Earth centered trajectory with a perigee radius of 10,000 km and zero inclination relative to the equator, the target values in \hat{c} are given by

$$\begin{pmatrix} r_f^* \\ \dot{r}_f^* \\ h_{xf}^* \\ h_{yf}^* \\ h_{zf}^* \end{pmatrix} = \begin{pmatrix} 10000 \text{ km} \\ 0 \text{ km/s} \\ 0 \\ 0 \\ 1 \end{pmatrix} \quad (11)$$

In principle, the problem is a two-point boundary value problem, where the trajectory constants are split and specified partly at t_0 and t_f , with both of these times being free and independent. The problem is difficult to solve because the trajectory dynamics are governed by a highly nonlinear vector differential equation of motion that needs to be solved between the specified endpoints. It has been determined that an efficient nonlinear root finding algorithm based on a multi-dimensional secant method is effective in solving this problem provided a reasonable estimate of the unknown parameter vector \mathcal{P} is given³. The gradient of \mathcal{E} with respect to \mathcal{P} is needed and it can be estimated numerically via finite central differences or by using the variational equations presented earlier.

Providing an initial estimate is based on using a bielliptic and patched conic transfer model⁴. This model provides a reasonable estimate on all of the parameters that form the parameter vector \mathcal{P} . This is followed by an iterative search until convergence is achieved.

Sensitivity Analysis

Having obtained a converged solution that is taken as a nominal trajectory, it is necessary to examine the sensitivity of this trajectory with respect to errors in the parameters used to define it. These errors include orbit determination errors of the spacecraft at a certain epoch, errors in the timing of key events such as maneuver start and end times, and errors associated with the maneuver itself, such as the thrust pointing attitude vector. Other error sources that should be accounted for in such a study include errors in the dynamic force model. In this section, the sensitivity matrix of the final constraint vector with respect to the parameters that define the trajectory is derived for both the impulsive and finite burn engine models. This matrix,

also known as the Jacobian matrix, can be used to determine which parameters most influence the final conditions. This analysis would then determine which parameters need to be controlled or monitored more accurately on these types of trajectories.

Sensitivity Analysis for the Impulsive Burn Model

For a converged trajectory uniquely described by the vectors \mathcal{P}_o and \mathcal{P}_i , a new 11 element parameter vector is defined as

$$\mathcal{P} = \left(\mathcal{P}_o \quad \mathcal{P}_i \quad t_i \quad \Delta \mathcal{V} \quad t_f \right)_{1 \times 11}^T \quad (12)$$

Where \mathcal{P}_o is the initial position vector at t_0 , \mathcal{P}_i is the initial velocity vector at t_0 , t_i is the coast time from t_0 , $\Delta \mathcal{V}$ is the Δv vector applied to the trajectory at t_i and t_f is the final time.

$\Delta \mathcal{V}$ can be decomposed into 3 components which are given by

$$\Delta \mathcal{V} = \begin{pmatrix} \Delta v \cos \alpha \cos \beta \\ \Delta v \sin \alpha \cos \beta \\ \Delta v \sin \beta \end{pmatrix}_{3 \times 1} \quad (13)$$

Where Δv is the scalar magnitude of the maneuver, α is the right ascension of the maneuver vector and β is declination of the maneuver vector

The state at t_i prior to the maneuver is \mathcal{P}_i , \mathcal{P}_i^- so that α and β are defined by

$$\alpha = \tan^{-1} \left(\frac{v_x}{v_y} \right) \quad (14)$$

$$\beta = \tan^{-1} \left(\frac{v_z}{\sqrt{v_x^2 + v_y^2}} \right) \quad (15)$$

Where v_x , v_y and v_z are the x, y, z components of \mathbf{v}_i^- .

The velocity vector after the maneuver is $\mathbf{v}_i^+ = \mathbf{v}_i^- + \Delta \mathbf{v}$. Eqn. 12, the parameter vector becomes

$$\mathbf{a} = \left(\rho_o \quad \rho_v \quad t_i \quad \Delta v \quad \alpha \quad \beta \quad t_f \right)_{1 \times 11}^T \quad (16)$$

The constraint vector, Eqn. 10, is redefined as a 2 x 1 vector

$$\mathbf{c} = \begin{pmatrix} r_{pf}^* - r_{pf} \\ i_f^* - i_f \end{pmatrix} \quad (17)$$

where i_f^* is the final target inclination and r_{pf}^* is the final target perigee radius.

The goal of the sensitivity analysis is to determine the gradient of \mathcal{E} with respect to \mathbf{a} . Since $\mathcal{E} = \mathcal{E}(\mathbf{a})$, the differential of \mathcal{E} is given by

$$\partial \mathcal{E} = \frac{\partial \mathcal{E}}{\partial \mathbf{a}} \partial \mathbf{a} \quad (18)$$

Eqn. 18 represents the Jacobian matrix of the system and its coefficients provide a linear estimate of the sensitivity of the final conditions or constraints with respect to perturbations in the parameter vector \mathbf{a} . This matrix is constructed by using the variational equations on the two segments of the trajectory; the first segment is from t_o to t_i and the second segment is from t_i to t_f . The Jacobian matrix is computed as

$$\frac{\partial \mathcal{E}}{\partial \mathbf{a}} = \frac{\partial \mathcal{E}}{\partial \mathbf{x}_f} \frac{\partial \mathbf{x}_f}{\partial \mathbf{a}} \quad (19)$$

where

$$\frac{\partial \mathcal{E}}{\partial \mathbf{x}_f} = \begin{pmatrix} \frac{\partial r_{pf}}{\partial \mathbf{x}_f} & \frac{\partial r_{pf}}{\partial \mathbf{v}_f} \\ \frac{\partial i_f}{\partial \mathbf{x}_f} & \frac{\partial i_f}{\partial \mathbf{v}_f} \end{pmatrix}$$

$$\frac{\partial \mathcal{E}}{\partial \mathbf{a}} = \left(\Phi(t_f, t_i) \begin{pmatrix} \mathbf{R}_i \\ \mathbf{R}_i \end{pmatrix} \begin{matrix} \rho_{io} \\ \mathbf{D}_{3 \times 3} \end{matrix} \begin{pmatrix} \mathbf{O}_{3 \times 3} \\ \mathbf{D}_{3 \times 3} \end{pmatrix} \begin{matrix} \mathbf{R}_f \\ \mathbf{R}_f \end{matrix} \right)_{6 \times 11}$$

$$\mathbf{D}_{3 \times 3} = \frac{\partial \mathbf{v}}{\partial (\Delta v, \alpha, \beta)}$$

In evaluating $\frac{\partial \mathcal{E}}{\partial \mathbf{x}_f}$, its components are readily evaluated since r_{pf} and i_f can be expressed explicitly as functions of \mathbf{v} and \mathbf{v} .

Sensitivity Analysis for the Finite Burn Model

Similarly, the parameter vector for the finite burn model is chosen to be

$$\mathbf{a} = \left(\rho_o \quad \rho_v \quad t_i \quad t_j \quad \alpha \quad \beta \quad t_f \right)_{1 \times 11}^T \quad (20)$$

Where t_j is the maneuver end time.

Using the same constraint vector as before, the Jacobian of the present system needs to account for the continuous burn segment that is integrated with the finite thrust value. The Jacobian matrix for this case takes the form

$$\frac{\partial \mathcal{E}}{\partial \mathbf{a}} = \frac{\partial \mathcal{E}}{\partial \mathbf{x}_f} \left(\mathbf{A}_{6 \times 10} \begin{matrix} \mathbf{R}_f \\ \mathbf{x}_f \end{matrix} \right)_{6 \times 11} \quad (21)$$

where

$$\mathbf{A}_{6 \times 10} = \left(\Phi_{fi} \right)_{6 \times 6} \begin{pmatrix} \Phi_{ji}^* \\ \mathbf{R}_j \end{pmatrix}_{6 \times 9} \mathbf{B}_{9 \times 10}$$

Note that Φ_{ji}^* is a submatrix partition of a 9 x 9 state transition matrix, $\Phi_{ji} = \Phi(t_j, t_o)$, evaluated along the finite burn segment with states \mathcal{P} , \mathcal{V} , m , α , β . Here, Φ_{ji}^* is Φ_{ji} with the last three rows and the seventh column removed and

$$B_{9 \times 10} = \begin{pmatrix} \Phi_{3 \times 6}^{\mathcal{P}} & \mathcal{R} & \Phi_{3 \times 3}^{\mathcal{V}} \\ \mathcal{O}_{3 \times 6} & \mathcal{O}_{3 \times 1} & I_{3 \times 3} \end{pmatrix}_{9 \times 10}$$

These relationships are then applied to a nominal transfer trajectory, and the Jacobian matrix of the system contains the sensitivity coefficients, to first order, of the final constraint conditions with respect to the injection parameters.

Sensitivity of a Nominal Impulsive Trajectory

As an example application of the perturbation analysis, a nominal Earth return lunar flyby trajectory has been determined. Table 1 lists the initial parameters that define this trajectory.

Table 1 - Transfer Trajectory Parameters

Parameter	Symbol	Value	Units
Epoch	t_o	2452263.430556	Julian Date
Semi-major axis	a_o	6578.137	km
Eccentricity	e	0.000	-
Inclination	i	28.500	deg
Ascending node	Ω	200.266	deg
Argument of periaapsis	ω	0.000	deg
True anomaly	ν	0.000	deg
Maneuver time	t_i	5308.248	sec
Δv magnitude	Δv	3.142770	km/s
Final time	t_f	7.460290	days
Final periaapsis radius	r_{pf}	8000	km
Final inclination	i_f	10	deg

Based on the parameters of Table 1, a new parameter vector that contains explicitly the

initial state and the maneuver parameters is tabulated in Table 2. Using the Jacobian matrix for this system, a perturbation to the initial parameter vector is examined. Table 3 lists the effect that this perturbation has on the final perigee radius and inclination of the Earth return trajectory.

Based on these results, it is clear that the final conditions are highly sensitive to most of the initial perturbations. In particular, the timing of the maneuver and the maneuver parameter values themselves are the most critical parameters associated with this trajectory. In the current configuration, an error of .1 deg in the right ascension of the maneuver will raise the perigee radius by nearly 1700 km. These results indicate that the maneuver has to be as accurate as possible. In contrast, the perturbation in the state parameters (position and velocity) just prior to the maneuver is not as critical. The uncertainty in the position and velocity of the spacecraft prior to the maneuver is available from the orbit determination process. However, this information is known prior to the maneuver itself so that the maneuver parameters can be recomputed based on the latest orbit determination data.

Table 2 - Converted Transfer Trajectory Parameters

Parameter	Symbol	Nominal Value	Units
Maneuver time	t_o	5308.248	sec
x position	x	-6170.913	km
y position	y	-2278.533	km
z position	z	0.000	km
x velocity	\mathcal{X}	2.3696	km/s
y velocity	\mathcal{Y}	-6.4175	km/s
z velocity	\mathcal{Z}	3.7143	km/s
Δv - magnitude	Δv	3.1427	km/s
Δv - right ascension	α	-69.842	deg
Δv - declination	β	28.499	deg

Table 3 - Perturbation Results

Perturbed Parameter	Symbol	Perturbation	$\Delta r_p(t_f)$ km	Δi_f deg
Maneuver time	δt_o	1 sec	930.799	2.928
x position	δx	.01 km	.894	0.385
y position	δy	.01 km	3.602	0.155
z position	δz	.01 km	-0.515	0.0017
x velocity	$\delta \dot{x}$.0001 km/s	49.200	-1.318
y velocity	$\delta \dot{y}$.0001 km/s	-32.267	3.894
z velocity	$\delta \dot{z}$.0001 km/s	25.307	-2.235
Δv – magnitude	$\delta \Delta v$.0001 km/s	244.024	-4.079
Δv – right ascension	$\delta \alpha$.1 deg	1691.745	5.328
Δv - declination	$\delta \beta$.1 deg	-15.879	-0.170

Applications for CubeSats on Deep Space Free Return Trajectories

As stated before, a deep space free return trajectory provides the capability for a spacecraft to observe a celestial object such as the moon, a comet, or asteroid for a brief period prior to returning to the Earth. The following is a list of possible CubeSat missions:

- CubeSats could be used to look for water on the surface of the Moon by using specialized sensors
- A constellation of CubeSats could be sent around the moon where a subset of these could land or impact the moon and the remainder could collect the data transmitted by the impactors or landers.
- One or several CubeSats can analyze the chemical composition of a comet's tail or the composition of near Earth asteroids.

A top level goal for any of these missions is to inspire students of all ages through hands on

participation in the program at any stage in the mission.

Based on these possible mission examples, it is clear that this class of picosatellites has the potential of being ideal space system for exploring the environment within several million kilometers of the Earth.

A Nominal Lunar CubeSat Mission

A mission plan for a lunar CubeSat mission is laid out in this section. The purpose of the mission is to use CubeSats to take pictures of both the Earth and the Moon while it is on a free return trajectory. Topics discussed include the mission timeline, the trajectory and propulsion considerations.

Mission Assumptions

During the analysis, several assumptions were made dealing with the location and time of the launch. Kennedy Space Center (KSC) was chosen as the launch site since it is a probable launch location. The time of launch was chosen to demonstrate the fact that this mission could happen immediately provided a launch vehicle was available. A true date of departure is hard to estimate since the logistics involved in getting student built satellites a ride on a launch vehicle are very complex. The mission will need to be designed around an available launch date and not the other way around. Based on the methodology used to identify a free return lunar flyby, such trajectories can be simulated by using the Astrogator Module of the Satellite ToolKit (STK)⁵.

Mission Scenario:

The mission scenario is based upon a launch from KSC on December 19, 2001 at 00:00:00 UTCG. Table 4 summarizes the

SSC01-III-3

entire mission from launch to return. The mission can be launched earlier provided the spacecraft is positioned in the correct orbit so that perigee occurs on December 19, 2001 at 23:48:08.13 UTCG. The insertion motor will have to fire at the specified time since the CubeSats will not have any fuel allocated for correction maneuvers. This mission, unlike typical missions, will have more of an insertion point of opportunity rather than a window.

Table 4 – Mission Timeline

Event	Day	Start Time (UTCG)	End Time (UTCG)
Launch from KSC and Parking Orbit Maneuvering	2001/12/19	00:00:00	23:48:08
Systems Check (Pictures Taken)	2001/12/20	00:00:00	01:00:00
Initial Orbit Determination	2001/12/20		
ΔV Applied	2001/12/20	01:16:35	01:16:35
CubeSats are Within 10,000 km of the Moon (Pictures Taken)	2001/12/23	21:49:00	01:27:00
CubeSats are Within 10,000 km of Earth (Data Downloaded)	2001/12/24	08:43:00	TBD

Figure 1 shows a two dimensional view of the nominal free return trajectory.

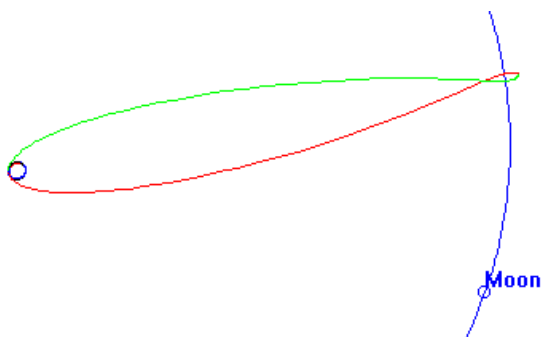


Figure 1 - STK Generated Free Return Trajectory

The periselene altitude of this trajectory is 3436 km above the moon's surface, and the perigee altitude of the return trajectory is 1624 km. The ΔV required for this particular mission from a 200 km parking orbit in LEO is 3.13 km/s.

Figures 2-4 represent snap shots at various times during CubeSat's flight. Note that the green line represents CubeSat's outbound trajectory, while the red line represents its inbound trajectory and the blue line represents the Moon's orbit.

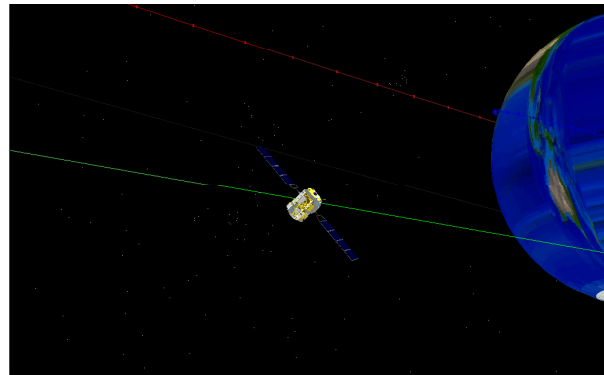


Figure 2 - CubeSat During Earth Departure

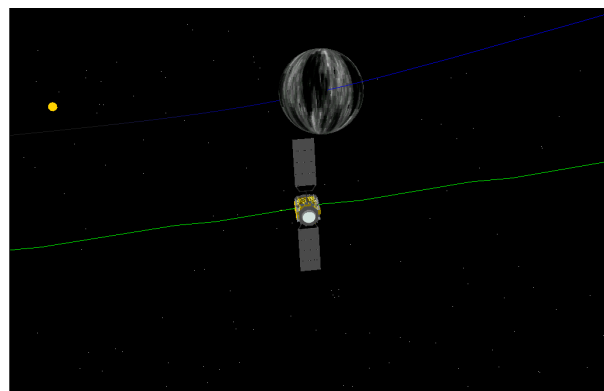


Figure 3 - CubeSats Approach the Moon

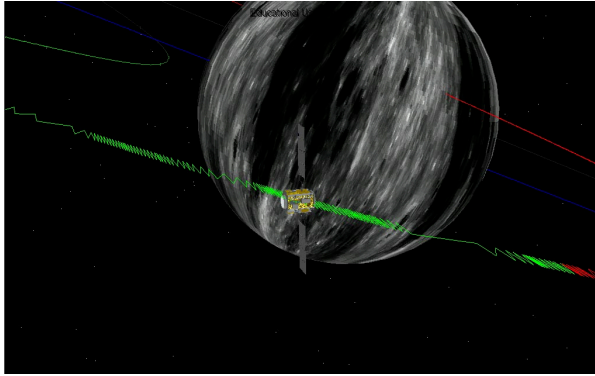


Figure 4 - CubeSats at Periselene

Booster

This mission by its very nature will require that only one maneuver be made in LEO. The accuracy of this maneuver is the most critical aspect of such a mission. Therefore, the booster or kick motor will be required to have a sophisticated onboard guidance system. Nevertheless, it is possible to examine the performance of currently available booster motors from a payload perspective.

Star motors⁶ are a class of small boosters that can be used for this purpose. An injection accuracy study would need to be performed on such a booster prior to choosing it as the nominal booster for this class of mission.

The payload mass that can be placed on the nominal translunar trajectory can be determined by the rocket equation

$$\Delta V = ISP * g * \ln\left(\frac{M_o}{M_o - M_f}\right) \quad (22)$$

Where ΔV is the known magnitude of the maneuver, g is the acceleration due to gravity, ISP is the specific impulse of the motor and M_o is the total mass of the spacecraft. The total mass of the spacecraft is explicitly defined by the following equation.

$$M_o = M_f + M_m + M_p + M_s \quad (23)$$

Where M_f is the mass of the fuel, M_m is the mass of the motor, M_p is the mass of the payload and M_s is the mass of the structure required to join the CubeSats with the motor.

Table 6 summarizes the results obtained from the motor sizing. All six motors examined are capable of producing the required ΔV , but do so with different parameters allowing anywhere from 3 to 45 CubeSats to be injected on the translunar trajectory. The number of CubeSats chosen for the mission will depend on how much payload and space is allocated by the launch vehicle. It is desirable to reach a balance between the maximization of the number of CubeSats and the total mass of the system. Increasing the number of CubeSats brings the cost of the overall program down but having too heavy of a system will limit the choice of launch vehicle.

Table 5 - ΔV Analysis Worksheet

STAR #	ISP (s)	Mf (kg)	Mp (kg)	Ms (kg)	Mm (kg)	Mo (kg)	g (m/s ²)	DV (km/s)
15	240	33.3389	5	4.5	2.4671	45.3059	9.81	3.1344
17	228	45.1322	5	4.35	5.3707	59.8529	9.81	3.1372
17A	286.2	69.6261	15	11.17	7.6589	103.4549	9.81	3.1384
20S	286.7	112.2635	30	17.5	7.4094	167.1729	9.81	3.1313
20	234	114.7583	20	8.75	10.5578	154.0660	9.81	3.1356
20A	286.5	273.1973	75	34	24.5878	406.7850	9.81	3.1296

Based on this, the STAR 20 motor, which has a successful track record, can place 16 CubeSats on the nominal trajectory. The combined mass of the booster and the CubeSats should be small enough to fly as an auxiliary payload. The STAR 15 on the other hand is also a reliable motor but is only capable of propelling 3 CubeSats. This option might be more viable in the event that the launch vehicle places an upper limit on the total payload launched to orbit.

Earth Return Trajectories to Asteroids and Comets

In a force field that includes the gravitational effect of the Earth and the Sun, there exist trajectories that have a hyperbolic energy relative to the Earth at departure, but return to the vicinity of the Earth several months later. These trajectories are solutions to the restricted three-body problem force field model and can be designed in a realistic Sun-Earth moon model that includes lunar and planetary perturbations. Like the free return lunar flyby trajectories, these trajectories require only one properly designed and executed injection maneuver from a low Earth parking orbit.

At the same time, knowing the orbital elements and the ephemeris of near Earth crossing comets or asteroids, it is possible to have a spacecraft intercept or flyby one of these objects. Such trajectories have been found and discussed in the literature^{7,8}. In these studies, flybys have been found for comets such as Encke, or asteroids such as Eros.

Due to the fact that the distance at which the flyby occurs is on the order of several million kilometers, it is expected that these trajectories will be highly sensitive to the launch parameters and will require greater accuracy than the lunar flyby mission. In contrast, the flyby body, being of a small mass compared to the Moon, will not provide a significant gravity assist or deflection maneuver to the spacecraft. Future work will examine the efficient computation of such trajectories, their stability and their sensitivity to injection parameter errors.

Conclusions

An efficient procedure has been described to compute Earth return lunar flyby trajectories applicable to passive spacecraft such as small satellites. Using the variational equations of motion for a spacecraft in the Earth-Moon system, the sensitivity of the Earth return trajectory to errors in the injection maneuver has been determined. Based on this analysis, the injection maneuver needs to be done with a reliable booster with onboard closed-loop guidance and possibly with the additional capability of providing a correction maneuver several hours after the main injection burn.

The possibility of designing and operating student built satellites on missions to the Moon and other near Earth celestial objects is intriguing because it extends the current envelop of where small student built satellite can operate. A mission that flies by the moon is relatively short (several days) yet will require careful planning since the encounter is brief and the trajectory dispersions on the return to the Earth could be large.

Several additional studies need to be completed prior to seriously considering such a mission. These include studies on the required spacecraft systems needed to operate autonomously at the flyby body, the communications requirements during the mission and the orbit determination requirements necessary to track the spacecraft.

There is no doubt such missions will take place in the future. Our goal is to make this happen as soon as practical and give the current generation of students the opportunity to work on the first student built spacecraft to operate in the vicinity of the Moon.

References

1. Ivashkin, V.V., and Typitsyn, N.N., "Use of the Moon's Gravitational Field to Inject a Space Vehicle into a Stationary Earth-Satellite Orbit," *Cosmic Research*, vol. 9, No.2, March-April 1997.
2. Ocampo, C.A., "Transfer to Earth Centered Orbits via Lunar Gravity Assist." Proceedings of the Applied Physics Laboratory conference on Missions to Small Bodies, May 2000.
3. Press W.H., Teukolsky S.A., Vetterling W.T., Flannery B.P., *Numerical Recipes In Fortran*, Cambridge University Press, 1992.
4. See Reference 2
5. More information on satellite ToolKit (STK) can be found at the following internet address: <http://www.stk.com/>
6. Morton Thiokol, *Space Rocket Motors Catalog*, June 2, 1986.
7. Farquhar R.W., Dunham D.W., S.C. Hsu, "Orbital Mechanics in the Sun-Earth-Moon System." Proceedings of the 2nd International Symposium on Spaceflight Dynamics, Damrstadt, Germany, October 1986.
8. Dunham D.W., Jen S.C., R.W. Farquhar, "Trajectories for Spacecraft Encounters with Comet Honda-Mrkos-Pajdusakova in 1996," *Acta Astronautica*, vol. 22, 1990

-
- 1
 - 2
 - 3
 - 4
 - 5
 - 6
 - 7
 - 8